9(2012) 95 – 110

Latin American Journal of Solids and Structures

www.lajss.org

A stress-displacement solution for a pressure tunnel with impermeable liner in elastic porous media

Abstract

Considering the effects of the changes of the pore water pressure around the opening, the construction sequence of the tunnel and the interaction between the liner and the surrounding geomaterial on the mechanical response of the tunnel and in conjunction with the analyses of the continuity and boundary conditions for the stress and displacement and hydraulic conditions, the elastic problem for a deep pressure tunnel with impermeable liner in a saturated elastic porous media that obeys Terzaghi's effective stress principle is investigated. The influences of the relative liner thickness and rigidity and the relative distance of the point under investigation to the tunnel axis on the stress-displacement fields for various combinations of the mechanical and geometric parameters are evaluated and discussed.

Keywords

tunnel, liner, porous media, relative liner thickness and rigidity, Terzaghi's effective stress principle.

M.B. Wang[a,*] **and G. Wang**[b]

[a] School of Civil Engineering, Ludong University, Yan'tai 264025 – P.R. China
[b] State Key Laboratory of Mine Disaster Prevention and Control, Shandong University of Science and Technology, Qingdao 266590 – P.R.China

Received 10 Jun 2011;
In revised form 04 Oct 2011

* Author email: sdrock2006@yahoo.cn

1 INTRODUCTION

With the development and upgrade of infrastructures, the demand for tunnel construction is increasing all over the world. Therefore, an extensive amount work has been done on the geomaterial-liner interaction of the tunnel based on elastic theory [7, 15].

When a tunnel is excavated under water-bearing geomaterial, seepage toward the tunnel takes place and the hydraulic head distributions around the tunnel are changed. Water inflow and water pressure controls are needed in the design, construction and exploitation of tunnels. Uncontrolled water behaviour may cause additional loads on the liner, mechanical instability, discomfort and adverse environmental impacts. Consequently, the loads imposed by the surrounding geomaterial, the fluid pressure inside the tunnel, and the changes in pore pressure in the surrounding geomaterial due to any leaks through the liner should be adequately considered in the liner design of a pressure tunnel. In addition, it is well-known that the internal pressure in tunnel results in an expansion of the liner which then transfers part of the load to the surrounding geomaterial. The pore water pressure in the surrounding geomaterial has a double effect: first it counteracts the expansion of the liner caused by the inside pressure,

and second it can change the stress field in the surrounding geomaterial around the tunnel decreasing effective stresses. Even though some of the effects of pore water pressure on tunnel support have been investigated [1, 3–6, 12–14, 16, 17], there are many aspects that require further scrutiny; in particular a criterion for tunnel support is needed where groundwater flow conditions are included.

One of the most important problems associated with tunneling is to determine the deformation produced by tunnel excavation. Even though this is a key aspect of tunneling, due to many complex factors affecting the solution, there are still a limited number of closed-form solutions than can be used to predict the deformation produced by tunnel excavation. Empirical or quasi-empirical methods are usually available. However, Chou and Bobet [8] note explicitly in their paper that empirical methods have significant shortcomings: (1) they have been developed or have been validated from a limited number of cases; (2) they should be applied only to tunnels that fall within the scope of the cases from which the method was developed; (3) only few soil and geometry parameters are taken into account; (4) they do not consider construction methods; and (5) they cannot give the complete solution of a tunnel with liner.

The present paper proposes an elastic stress-displacement solution for a deep pressure tunnel with impermeable liner excavated in a saturated elastic porous geomaterial that obeys Terzaghi's effective stress principle [2, 18], as shown in Fig. 1. In all the analyses the following assumptions are made:(1) the geomaterial and the liner are always elastic; (2) the permeability of the geomaterial is homogeneous and isotropic; (3) the groundwater field is a steady-flow seepage field; (3) the cross-section of the tunnel is circular; (4) plane strain conditions are applicable at any cross-section of the tunnel; (5) the tunnel is deep enough so that the stress distribution before excavation is homogeneous. Even though some assumptions may be too restrictive, the method has the following advantages: (1) it is simple to use; (2) it can properly model the tunnel construction sequence; (3) it can be used for preliminary design, which facilitates a more advanced or detailed modeling of the tunnel.

2 PROBLEM STATEMENT

Consider an infinite elastic plane *oxy* (geomaterial made in elastic porous material, or Region 1) that is homogeneous, except for the presence of a deep circular lined tunnel subjected to uniform internal pressure $-q_o$ (with q_o a positive number and tensile stresses are considered as positive in the work), or Region 2 (see Fig. 1). The elastic constants of the geomaterial are denoted by G_1 (shear modulus) and γ_1 (Poisson's ratio), and the polar coordinates in the *oxy* plane by r and θ. It is assumed that the tunnel-axis is aligned with the direction of the third out-of-plane z-axis. The inner and outer radii of the liner are denoted by a and t, respectively, and its elastic constants by G_2 and γ_2. Axi-symmetry conditions for geometry and loading will be assumed (i.e., gravity will be disregarded), so the problem in Fig.1 is representative of the case of a deep tunnel excavated in elastic geomaterial subject to uniform initial stresses. Here, we define t/a as the relative thickness of the liner and the relative rigidity of the liner,

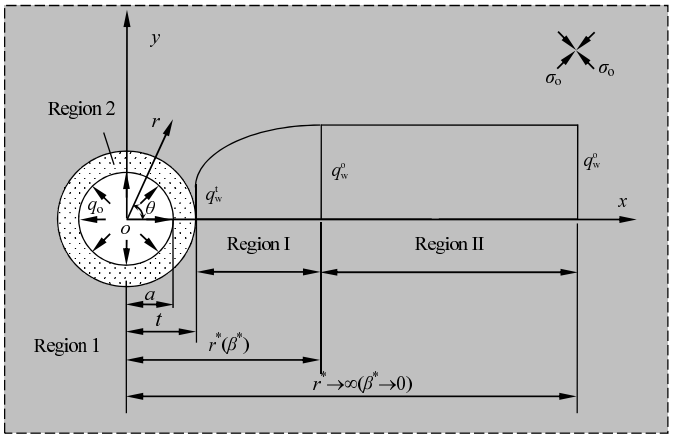

Figure 1 Lined circular tunnel subjected to total stresses (including in situ stress and water pore pressure).

which is defined as

$$\Gamma = \frac{G_2}{G_1} \tag{1}$$

In addition, as discussed in the main text, a dimensionless variable β is defined in terms of the outer radius of the liner t and the radial distance r to the tunnel axis, as follows

$$\beta = \frac{t}{r} \tag{2}$$

Also, the solution is expressed in terms of the two Lame's elastic parameters, λ and G respectively, that are related to the Young's modulus E and the Poisson's ratio γ of the liner and the geomaterial as follows

$$G = \frac{E}{2(1+\gamma)} \tag{3}$$

and

$$\lambda = \frac{E\gamma}{(1+\gamma)(1-2\gamma)} \tag{4}$$

Prior to excavation, the total stresses and the pore water pressure in the geomaterial are uniform and equal to $-\sigma_o$ and $-q_w^o$, respectively. The tunnel is then excavated and water is drained from inside the tunnel, leading to the non-uniform pore water pressure distribution shown in Fig.1, where $q_w = -q_w^t$ at the outer boundary of the liner and $q_w = -q_w^o$ at and beyond the radial distance $r = r^*$. The pore water pressure distribution is depicted by Regions I and II in Fig.1, respectively. By using Terzaghi's effective stress principle, the total stress can be decomposed into effective stresses and pore water pressure and the equation can be written in matrix notation as

$$\sigma = \sigma' + q_w \tag{5}$$

where σ represents a component of total normal stress, σ' the corresponding component of effective normal stress, and q_w the pore water pressure.

3 THE CLOSED-FORM FULL FIELD ELASTIC SOLUTION

According to Eq.(2), the radial distance r can therefore be expressed as follows

$$r = \frac{t}{\beta} \tag{6}$$

In view of the relationship (6), the first derivation of an arbitrary function with respect to the variable r, can be equally expresssed in terms of the derivative of the same function with respect to the variable β, i.e.,

$$\frac{d(\,)}{dr} = -\frac{\beta^2}{t}\frac{d(\,)}{d\beta} \tag{7}$$

similarly, the second derivative of an arbitrary function with respect to the variable r results

$$\frac{d^2(\,)}{dr^2} = \frac{2\beta^3}{t^2}\frac{d(\,)}{d\beta} + \frac{\beta^4}{t^2}\frac{d^2(\,)}{d\beta^2} \tag{8}$$

Firstly, the solution for pore water pressure is discussed. The differential equation in a steady flow field can be expressed in terms of the pore water pressure q_w and the radial distance r as follows [10]

$$\frac{d^2q_w}{dr^2} + \frac{1}{r}\frac{dq_w}{dr} = 0 \tag{9}$$

In view of the transformation (6), Eq.(9) can be equally expressed in terms of β as follows

$$\frac{d^2q_w}{d\beta^2} + \frac{1}{\beta}\frac{dq_w}{d\beta} = 0 \tag{10}$$

The general solution of Eq.(10) is obtained as follows

$$q_w(\beta) = A_1 + A_2 \ln\beta \tag{11}$$

where A_1 and A_2 are integration constants.

In reference to Fig.1, the values of the pore water pressure at the distances $r = t$ (or $\beta = 1$) and $r = r^*$ are as follows, respectively

$$q_w = -q_w^t \quad \beta = 1 \tag{12}$$

and

$$q_w = -q_w^o \quad \beta = \beta^* \tag{13}$$

By substituting Eqs.(12) and (13) into Eq.(11), the coefficients A_1 and A_2 in Eq.(11) are determined as

$$A_1 = -q_w^t \tag{14}$$

and

$$A_2 = \frac{q_w^t - q_w^o}{\ln \beta^*} \tag{15}$$

Consequently, the solutions for the pore water pressure in Regions I and II result in as follows, respectively

$$q_w^I(\beta) = -q_w^t + (q_w^t - q_w^o)\frac{\ln \beta}{\ln \beta^*} \qquad \beta^* \le \beta \le 1 \tag{16}$$

and

$$q_w^{II}(\beta) = -q_w^o \qquad 0 \le \beta \le \beta^* \tag{17}$$

Next, we discuss the derivation of the solution for displacements and stresses. Considering Eqs.(6) and (7), the differential equation of equilibrium for the axisymmetric problem can be expressed as

$$\frac{d\sigma_r}{d\beta} - \frac{\sigma_r - \sigma_\theta}{\beta} = 0 \tag{18}$$

In addition, the radial strain ϵ_r and ϵ_θ can be equally expressed in terms of the radial displacement u_r and the variable β as follows, respectively

$$\varepsilon_r = -\frac{\beta^2}{t}\frac{\mathrm{d}u_r}{\mathrm{d}\beta} \tag{19}$$

and

$$\varepsilon_\theta = \frac{\beta}{a}u_r \tag{20}$$

According to Terzaghi's effective stress principle, only the effective components of normal stresses induce mechanical deformation, therefore, the elastic stress-strain relationships, as defined by the theory of elasticity, may be revised as

$$\varepsilon_r^1 = \frac{1}{E}\{(\sigma_r - q_w) - \gamma[(\sigma_\theta - q_w) + (\sigma_z - q_w)]\} \tag{21}$$

$$\varepsilon_\theta^1 = \frac{1}{E}\{(\sigma_\theta - q_w) - \gamma[(\sigma_r - q_w) + (\sigma_z - q_w)]\} \tag{22}$$

$$\varepsilon_z^1 = \frac{1}{E}\{(\sigma_z - q_w) - \gamma[(\sigma_\theta - q_w) + (\sigma_r - q_w)]\} \tag{23}$$

where, ε_r^1, ε_θ^1 and ε_z^1 denote the total strains including the components prior to excavation. Similarly, prior to excavation, between the strains, defined by ε_r^o, ε_θ^o and ε_z^o, and the stresses by σ_r^o, σ_θ^o and σ_z^o, the following relationships yield

$$\varepsilon_r^o = \frac{1}{E}\{(\sigma_r^o + q_w^o) - \gamma[(\sigma_\theta^o + q_w^o) + (\sigma_z^o + q_w^o)]\} \tag{24}$$

$$\varepsilon_\theta^o = \frac{1}{E}\left\{(\sigma_\theta^o + q_w^o) - \gamma\left[(\sigma_r^o + q_w^o) + (\sigma_z^o + q_w^o)\right]\right\} \tag{25}$$

$$\varepsilon_z^o = \frac{1}{E}\left\{(\sigma_z^o + q_w^o) - \gamma\left[(\sigma_\theta^o + q_w^o) + (\sigma_r^o + q_w^o)\right]\right\} \tag{26}$$

Hence, the incremental strains ε_r, ε_θ and ε_z may be obtained as follows

$$\begin{aligned}\varepsilon_r &= \varepsilon_r^1 - \varepsilon_r^o \\ &= \frac{1}{E}\left\{(\sigma_r - q_w) - (\sigma_r^o + q_w^o) - \gamma\left[(\sigma_\theta - q_w) - (\sigma_\theta^o + q_w^o) + (\sigma_z - q_w) - (\sigma_z^o + q_w^o)\right]\right\}\end{aligned} \tag{27}$$

$$\begin{aligned}\varepsilon_\theta &= \varepsilon_\theta^1 - \varepsilon_\theta^o \\ &= \frac{1}{E}\left\{(\sigma_\theta - q_w) - (\sigma_\theta^o + q_w^o) - \gamma\left[(\sigma_r - q_w) - (\sigma_r^o + q_w^o) + (\sigma_z - q_w) - (\sigma_z^o + q_w^o)\right]\right\}\end{aligned} \tag{28}$$

$$\begin{aligned}\varepsilon_z &= \varepsilon_z^1 - \varepsilon_z^o \\ &= \frac{1}{E}\left\{(\sigma_z - q_w) - (\sigma_z^o + q_w^o) - \gamma\left[(\sigma_\theta - q_w) - (\sigma_\theta^o + q_w^o) + (\sigma_r - q_w) - (\sigma_r^o + q_w^o)\right]\right\}\end{aligned} \tag{29}$$

In terms of Eqs.(27)-(29), for the special case of plane strain, i.e., $\varepsilon_z = 0$, the following expressions results in

$$(\sigma_r - q_w) + (\sigma_o - q_w^o) = (\lambda + 2G)\varepsilon_r + \lambda\varepsilon_\theta \tag{30}$$

$$(\sigma_\theta - q_w) + (\sigma_o - q_w^o) = (\lambda + 2G)\varepsilon_\theta + \lambda\varepsilon_r \tag{31}$$

$$(\sigma_z - q_w) + (\sigma_o - q_w^o) = \lambda(\varepsilon_r + \varepsilon_\theta) \tag{32}$$

wherein, $\sigma_r - q_w$, $\sigma_\theta - q_w$ and $\sigma_z - q_w$ represent the effective components of radial, tangential and axial stresses, respectively, while $\sigma_o - q_w^o$ represent the initial effective in situ stress.

By substituting Eqs.(30) and (31) together with Eqs.(19) and (20) into Eq.(18), the following differential equation representing the equilibrium condition in terms of the displacements is obtained

$$\beta^2 \frac{d^2 u_{r1}}{d\beta^2} + \beta \frac{du_{r1}}{d\beta} - u_{r1} - \frac{t}{\lambda_1 + 2G_1}\frac{dq_w}{d\beta} = 0 \tag{33}$$

where, the second subscripts 1 is related to the components in the surrounding geomaterial. For region I, noting Eq.(16), the solution of Eq.(33) gives the following expression for the radial displacement

$$u_{r1}^I(\beta) = \frac{A_1^I}{\beta} + A_2^I\beta + \frac{t\left(q_w^o - q_w^t\right)}{2\left(\lambda_1 + 2\mathrm{G}_1\right)}\frac{\ln\beta}{\beta\ln\beta^*} \tag{34}$$

where, the superscript I is related to the components in the region I of the surrounding geomaterial. In addition, based on Eqs.(30) and (31), the radial and tangential stresses are obtained as, respectively

$$\sigma_{r1}^{I}(\beta) = -\sigma_o + \left(q_w^o - q_w^t\right) + \frac{2(\lambda_1 + G_1)}{t} A_1^I - \frac{2G_1}{t}\beta^2 A_2^I - \frac{q_w^o - q_w^t}{2\ln\beta^*}\left(1 + \frac{2G_1}{\lambda_1 + 2G_1}\ln\beta\right) \tag{35}$$

and

$$\begin{aligned}\sigma_{\theta 1}^{I}(\beta) = -\sigma_o + \left(q_w^o - q_w^t\right) + \frac{2(\lambda_1+G_1)}{t} A_1^I + \frac{2G_1}{t}\beta^2 A_2^I \\ -\frac{q_w^o - q_w^t}{2\ln\beta^*}\left(\frac{\lambda_1}{\lambda_1+2G_1} + \frac{2G_1}{\lambda_1+2G_1}\ln\beta\right)\end{aligned} \tag{36}$$

As for region II, noting Eq.(17), the following expressions for the displacement and stresses result in

$$u_{r1}^{II}(\beta) = \frac{A_1^{II}}{\beta} + A_2^{II}\beta \tag{37}$$

$$\sigma_{r1}^{II}(\beta) = -\sigma_o + \left(q_w^o - q_w^t\right) + \frac{2(\lambda_1 + G_1)}{t} A_1^{II} - \frac{2G_1}{t}\beta^2 A_2^{II} \tag{38}$$

$$\sigma_{\theta 1}^{\mathrm{B}}(\beta) = -\sigma_o + \left(q_w^o - q_w^t\right) + \frac{2(\lambda_1 + G_1)}{t} A_1^{II} + \frac{2G_1}{t}\beta^2 A_2^{II} \tag{39}$$

where, the superscript II is related to the components in the region II of the surrounding geomaterial.

In reference to Fig.1, the boundary or continuity conditions at the distances $r = t$ (or $\beta = 1$), $r \to \infty$ (or $\beta \to 0$) and $r = r^*$ (or $\beta = \beta^*$) are summarized as

$$\sigma_{r1}^{I} = -\left(q_s + q_w^t\right) \quad \beta = 1 \tag{40}$$

$$\sigma_{r1}^{II} = -\sigma_o \quad \beta = 0 \tag{41}$$

$$\sigma_{r1}^{I} = \sigma_{r1}^{II} \quad \beta = \beta^* \tag{42}$$

$$u_{r1}^{I} = u_{r1}^{II} \quad \beta = \beta^* \tag{43}$$

where, q_s denotes the normal pressure along the interface between the liner and the surrounding geomaterial for the case that the liner is impermeable. Eqs.(40) through (43) – with σ_{r1}^{I}, σ_{r1}^{II}, u_{r1}^{I} and u_{r1}^{II} defined by Eqs.(35), (38), (34) and (37), respectively – conform a system of four algebraic equations to solve four unknowns, the variables A_1^I, A_2^I, A_1^{II} and A_2^{II}, as follows

$$A_1^I = \frac{t}{2(\lambda_1 + 2G_1)}\left(q_w^t - q_w^o\right)\left(1 - \frac{1}{2\ln\beta^*}\right) \tag{44}$$

$$A_2^I = \frac{t}{2G_1}\left(q_s + q_w^t - \sigma_o\right) + \frac{t}{2(\lambda_1 + 2G_1)}\left(q_w^t - q_w^o\right)\left(\frac{1}{2\ln\beta^*} - 1\right) \tag{45}$$

$$A_1^{II} = 0 \tag{46}$$

$$A_2^{II} = \frac{t}{2G_1}\left(q_s + q_w^t - \sigma_o\right) + \frac{t}{2(\lambda_1 + 2G_1)}\left(q_w^t - q_w^o\right)\left[\frac{1}{2\ln\beta^*} - 1 - \frac{1}{2(\beta^*)^2\ln\beta^*}\right] \tag{47}$$

In summary, substituting Eqs.(44) and (45) into Eqs.(34)-(36) and Eqs.(46) and (47) into Eqs.(37)-(39), respectively, the final expressions for the displacements and stresses for regions I and II are obtained as follows

$$u_{r1}^{I}(\beta) = \frac{t}{2G_1}\left(q_s + q_w^t - \sigma_o\right)\beta - \frac{t}{4\left(\lambda_1 + 2G_1\right)}\frac{q_w^t - q_w^o}{\beta \ln \beta^*}\left[2\ln\beta + \left(1-\beta^2\right)\left(1 - 2\ln\beta^*\right)\right] \tag{48}$$

$$\sigma_{r1}^{I}(\beta) = -\sigma_o - \left(q_s + q_w^t - \sigma_o\right)\beta^2 + \frac{2G_1}{4\left(\lambda_1 + 2G_1\right)}\frac{q_w^t - q_w^o}{\ln \beta^*}\left[2\ln\beta + \left(1-\beta^2\right)\left(1 - 2\ln\beta^*\right)\right] \tag{49}$$

$$\sigma_{\theta 1}^{I}(\beta) = -\sigma_o + \left(q_s + q_w^t - \sigma_o\right)\beta^2 + \frac{2G_1}{4\left(\lambda_1 + 2G_1\right)}\frac{q_w^t - q_w^o}{\ln \beta^*}\left[2\ln\beta - 2 + \left(1+\beta^2\right)\left(1 - 2\ln\beta^*\right)\right] \tag{50}$$

$$u_{r1}^{II}(\beta) = \frac{t}{2G_1}\left(q_s + q_w^t - \sigma_o\right)\beta - \frac{t}{4\left(\lambda_1 + 2G_1\right)}\frac{q_w^t - q_w^o}{\left(\beta^*\right)^2 \ln \beta^*}\beta\left[1 - \left(\beta^*\right)^2 + 2\left(\beta^*\right)^2 \ln\beta^*\right] \tag{51}$$

$$\sigma_{r1}^{II}(\beta) = -\sigma_o - \left(q_s + q_w^t - \sigma_o\right)\beta^2 + \frac{2G_1}{4\left(\lambda_1 + 2G_1\right)}\frac{q_w^t - q_w^o}{\left(\beta^*\right)^2 \ln \beta^*}\beta^2\left[1 - \left(\beta^*\right)^2 + 2\left(\beta^*\right)^2 \ln\beta^*\right] \tag{52}$$

$$\sigma_{\theta 1}^{II}(\beta) = -\sigma_o + \left(q_s + q_w^t - \sigma_o\right)\beta^2 - \frac{2G_1}{4\left(\lambda_1 + 2G_1\right)}\frac{q_w^t - q_w^o}{\left(\beta^*\right)^2 \ln \beta^*}\beta^2\left[1 - \left(\beta^*\right)^2 + 2\left(\beta^*\right)^2 \ln\beta^*\right] \tag{53}$$

The above expressions for radial and tangential stresses correspond to total stresses. According to Terzaghi's effective stress principle (Eq.(5)), the effective radial and tangential stresses for regions I and II, are computed as follows

$$\sigma_r'(\beta) = \sigma_r(\beta) - q_w(\beta) \tag{54}$$

$$\sigma_\theta'(\beta) = \sigma_\theta(\beta) - q_w(\beta) \tag{55}$$

By making $q_w^t = q_w^o = 0$ in Eqs.(48)-(53), the classical Lamé's solution can be recovered. In this case, the total and effective stresses are the same and the solution for radial displacement, radial stress and tangential stress, result to be, respectively

$$u_{r1}(\beta) = \frac{t}{2G_1}\left(q_s - \sigma_o\right)\beta \tag{56}$$

$$\sigma_{r1}(\beta) = -\sigma_o - \left(q_s - \sigma_o\right)\beta^2 \tag{57}$$

$$\sigma_{\theta 1}(\beta) = -\sigma_o + \left(q_s - \sigma_o\right)\beta^2 \tag{58}$$

For another special case that the pore water pressure distribution in the surrounding geomaterial is uniform, by considering $q_w^t = q_w^o$ in Eqs.(48)-(53), the following expressions for displacement and stresses are obtained

$$u_{r1}(\beta) = \frac{t}{2G_1}\left(q_s + q_w^o - \sigma_o\right)\beta \tag{59}$$

$$\sigma_{r1}(\beta) = -\sigma_o - (q_s + q_w^o - \sigma_o)\beta^2 \tag{60}$$

$$\sigma_{\theta 1}(\beta) = -\sigma_o + (q_s + q_w^o - \sigma_o)\beta^2 \tag{61}$$

For this case there is no distinction between regions I and II, in terms of Eqs.(16) and (17), the solution for the pore water pressure is

$$q_w(\beta) = q_w^I(\beta) = q_w^{II}(\beta) = -q_w^o \tag{62}$$

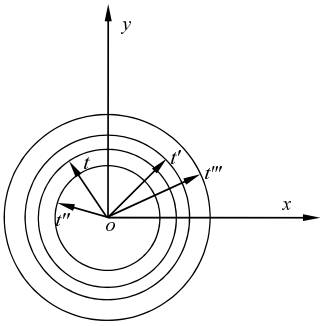

Figure 2 Model for tunnel construction.

Finally, the solution for the support pressure q_s is discussed below. It is assumed that the radii of the opening immediately after excavation, after the elastic deformation finishes and before the liner is installed, are t''', t'' and t', respectively. The construction sequence of the tunnel is modeled with regard to Fig.2. Then, we define

$$\eta = \frac{t' - t''}{t'} \tag{63}$$

as the relative radius misfit between the surrounding geomaterial and the liner. This misfit is assumed of the order of the admissible strains in linear elasticity.

Based on Kirsch's solution [11] and Eq.(48), t'' is expressed as follows

$$t'' = t'''\left[1 - \frac{\sigma_o}{2G_1}\right] \tag{64}$$

The case of $\eta = 0$ means that the liner is installed after the elastic deformation finishes, and $\eta = \eta_{max}$ means that the region of $r \le t'''$ in the surrounding geomaterial is replaced by the liner. Thus, η_{max} can be written in the following form

$$\eta_{\max} = \frac{t''' - t''}{t'''} = \frac{\sigma_o}{2G_1} \tag{65}$$

Substituting (65) into (64) yields the following relation

$$t'' = (1 - \eta_{\max})\, t''' \tag{66}$$

Next, the elastic deformation rate of the surrounding geomaterial is defined by

$$\delta = \frac{t''' - t'}{t''' - t''} \times 100\% \tag{67}$$

Taking advantage of Eq.(66), δ can be rewritten

$$\delta = \frac{1}{\eta_{\max}} \left(1 - \frac{t'}{t'''} \right) \times 100\% \tag{68}$$

Inserting Eqs.(65), (66) and (68) into Eq.(63) gives

$$\eta = \frac{(1-\delta)\,\eta_{\max}}{1 - \delta\eta_{\max}} \tag{69}$$

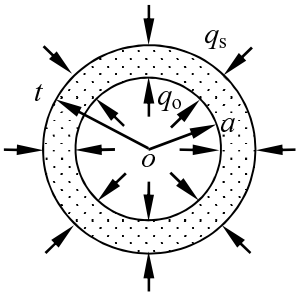

Figure 3 Mechanical model for the liner.

In terms of the Lamé's solution and Eq.(6), the stresses and displacement in the liner may be equally written as follows (see Fig.3)

$$\sigma'_{r2}(\beta) = \sigma_{r2}(\beta) = -\frac{\beta^2 - 1}{\frac{t^2}{a^2} - 1} q_o - \frac{1 - \frac{a^2}{t^2}\beta^2}{1 - \frac{a^2}{t^2}} q_s \tag{70}$$

$$\sigma'_{\theta 2}(\beta) = \sigma_{\theta 2}(\beta) = \frac{\beta^2 + 1}{\frac{t^2}{a^2} - 1} q_o - \frac{1 + \frac{a^2}{t^2}\beta^2}{1 - \frac{a^2}{t^2}} q_s \tag{71}$$

$$u_{r2}(\beta) = \frac{1}{2G_2} \frac{\beta}{t} \left[\frac{(1-2\gamma_2)\,\frac{a^2}{\beta^2} + a^2}{1 - \frac{a^2}{t^2}} q_o - \frac{(1-2\gamma_2)\,\frac{t^2}{\beta^2} + a^2}{1 - \frac{a^2}{t^2}} q_s \right] \tag{72}$$

Furthermore, it is noted that the liner will be installed when the tunnel partially deforms. Hence, the following relationship results in

$$u^I_{r1}(1)\big|_{\sigma_o = 0} = u_{r2}(1) + \eta t \tag{73}$$

By substituting Eqs.(48) and (72) into Eq.(73), the expression of q_s is obtained

$$q_s = \frac{2\left(1-\gamma_2\right)a^2 q_o + \left(2\eta G_2 - \Gamma q_w^t\right)\left(t^2-a^2\right)}{\left(1-2\gamma_2+\Gamma\right)t^2 + \left(1-\Gamma\right)a^2} \tag{74}$$

In terms of Eq.(48), the displacement along the interface between the liner and the surrounding geomaterial may also be written in a explicit form as follows

$$\begin{aligned} u_{r1}^I(1) = {} & \frac{\eta t\Gamma\left(t^2-a^2\right)}{(1-2\gamma_2+\Gamma)t^2+(1-\Gamma)a^2} + \frac{t}{2G_1}\frac{(1-2\gamma_2)a^2+a^2}{(1-2\gamma_2+\Gamma)t^2+(1-\Gamma)a^2}q_o \\ & + \frac{t}{2G_1}\frac{(1-2\gamma_2)t^2+a^2}{(1-2\gamma_2+\Gamma)t^2+(1-\Gamma)a^2}q_w^t - \frac{t}{2G_1}\sigma_o \end{aligned} \tag{75}$$

where and hereafter, $u_{r1}^I(1)$ denotes the support displacement corresponding to the case that the liner is impermeable.

In terms of Eqs.(74) and (75), it may be found that the pore water pressure distribution in the surrounding geomaterial has significant influences on the support pressure q_s and displacement $u_{r1}^I(1)$. The support pressure q_s and displacement $u_{r1}^I(1)$ may decrease with increasing the pore water pressure q_w^t along the outer boundary of the liner and the reverse trend may occur if to decrease the pore water pressure q_w^t. As for the internal water pressure q_o, it may be found that the support pressure q_s increases with increasing the internal water pressure q_o. However, the support displacement $u_{r1}^I(1)$ decreases with increasing the internal water pressure q_o.

4 NUMERICAL RESULTS AND DISCUSSIONS

In this Section, in order to illustrate the appllication of the obtained solution, we take $\gamma_1 = \gamma_2 = 0.3$, $\delta = 0$, $G_1/\sigma_o = 10^3$, $q_w^o = 0.5\sigma_o$, $q_w^t = 0.025\sigma_o$, $q_o = 0.05\sigma_o$ and $r^* = 5a^2/t$.

The variations of the normalized support pressure (q_s/σ_o) and displacement $(G_1 u^I r1(1)/(\sigma_o a))$ with relative liner rigidity for various relative liner thicknesses are depicted in Figs.4 and 5. It is seen that in general the varying trend of the support pressure with respect to relative liner rigidity for various liner thicknesses is similar to that of the support displacement. Namely, both of the support pressure and displacement monotonically increase with increasing liner rigidity and thickness. From Figs.4 and 5, it is further seen that in the range of $1 \le \Gamma \le 200$, the influences of the liner rigidity and thickness on the support pressure and displacement are significant. However, in the range of $200 < \Gamma \le 800$, the variations of the support pressure and displacement with various values of Γ or t/a become insignificant. Finally, when $800 < \Gamma$, the variations of the support pressure and displacement are almost independent of the values of Γ and t/a.

In Figs.6 and 7, we illustrate the variations of the normalized effective stresses in the liner and the surrounding geomaterial with relative liner thickness (t/a) and distance to the tunnel axis (r/a) when $\Gamma = 10$ [9, 15]. It is found from Fig.6 that at first the effective radial stress increases with increasing distance to the tunnel axis and then holds a maximum value when the distance to the tunnel axis reaches a certain magnitude for a specific liner thickness. Moreover, it is observed that with increasing relative liner thickness these aforementioned maximum

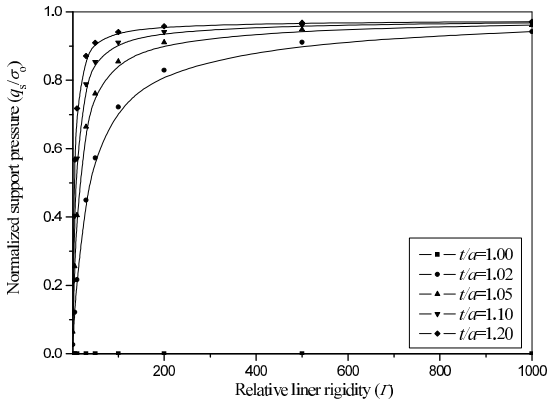

Figure 4 Variations of the normalized support pressure (q_s/σ_o) with the relative liner rigidity (Γ) for various relative liner thicknesses (t/a).

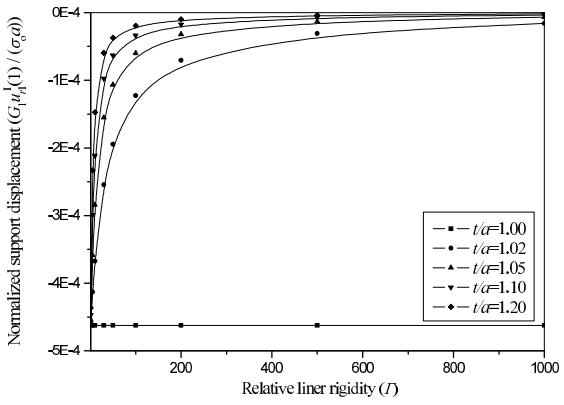

Figure 5 Variations of the normalized support displacement ($G_1 u^I_{r1}(1)/(\sigma_o a)$) with the relative liner rigidity (Γ) for various relative liner thicknesses (t/a).

values of $\sigma_r^{'}$ increases and the corresponding position of the points holding a maximum value in the surrounding geomaterial gradually approaches to the outer boundary of the liner. When the distance to the tunnel is further increased, $\sigma_r^{'}$ may also gain a minimum value when those points under investigation in the surrounding geomaterial reach the position of r^* (or β^*).

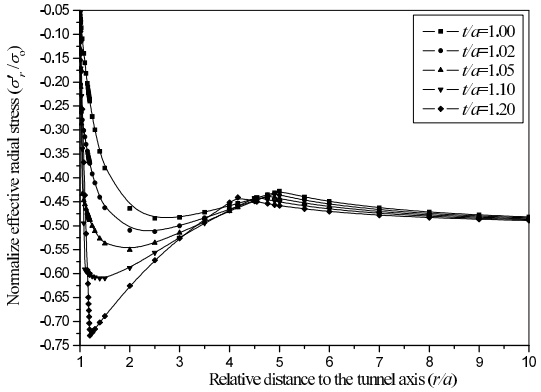

Figure 6 Variations of normalized radial stress ($\sigma_r^{'}/(\sigma_o)$) with relative distance to the tunnel axis (r/a) for various relative liner thicknesses (t/a) when Γ = 10.

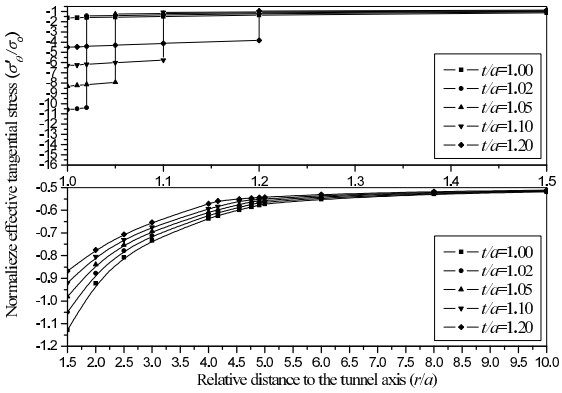

Figure 7 Variations of normalized tangential stress ($\sigma_\theta^{'}/(\sigma_o)$) with relative distance to the tunnel axis (r/a) for various relative liner thicknesses (t/a) when Γ = 10.

The variations of the normalized tangential stress $\sigma_\theta^{'}/\sigma_o$ versus the relative distance to the tunnel axis with different relative liner thicknesses when Γ = 10 are shown in Fig.7. In contrast to the varying trend of the normalized radial stress, it is found that at first in the liner the normalized tangential stress decreases with increasing the relative distance to the tunnel axis and then along the interface between the liner and the surrounding geomaterial there is a jump or discontinuity in the tangential stress, i.e., the tangential stress in the liner

is much higher than that in the surrounding geomaterial. And the jump values decrease with increasing relative liner thickness. As for the tangential stress in the surrounding geomaterial, it is found that $\sigma_\theta^{'}/\sigma_o$ also decreases with increasing r/a and t/a. In addition, compared with the variation of the radial stress at $r = r^*$, it may be observed that the tangential stress does not exist extremum property at $r = r^*$.

By comparing Figs.8 and 9 with Figs.6 and 7, an interesting phenomenon is observed that the variations of the normalized effective stresses with relative liner rigidity are similar to those with relative liner thickness. Moreover, it may be found from Figs. 6 and 8 that around the position of r^* the fluctuation range of the minimum value of $\sigma_r^{'}$ with relative liner rigidity compared with relative liner thickness is large, and that for a certain liner rigidity the distance to the tunnel axis of those points holding a minimum value of $\sigma_r^{'}$ decreases with increasing the liner thickness. However, for a certain liner thickness the position of those points holding a minimum value of $\sigma_r^{'}$ is almost fixed.

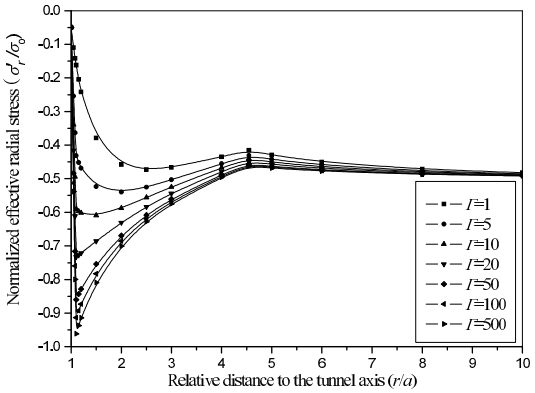

Figure 8 Variations of normalized radial stress ($\sigma_r^{'}(\sigma_o)$) with relative distance to the tunnel axis (r/a) for various relative liner rigidities (Γ) when t/a = 1.10.

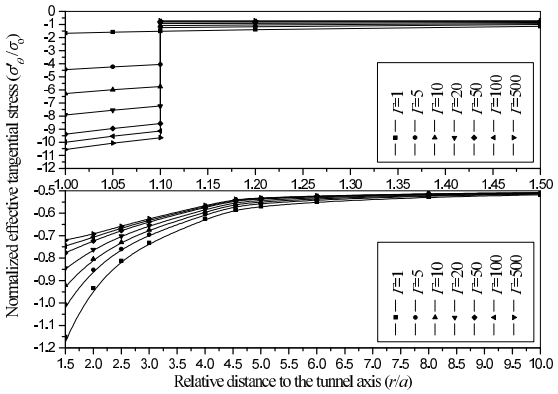

Figure 9 Variations of normalized tangential stress ($\sigma_\theta^{'}/(\sigma_o)$) with relative distance to the tunnel axis (r/a) for various relative liner rigidities (Γ) when t/a = 1.10.

It is also seen from Figs.6-9 that in a range about $1 \le r/a \le r^*/a$ the influences of the liner thickness and rigidity and the distance to the tunnel axis on the stress fields are significant and when $r^*/a < r/a \le 8$ the influences become trivial. As for $r/a > 8$, the variations of the stress fields are almost independent of the values of r/a, t/a and Γ.

The variations of the normalized radial displacement with relative liner thickness and distance to the tunnel axis when Γ = 10 are depicted in Fig.10. It is seen that in general the normalized radial displacement decreases monotonically with increasing relative liner thickness and distance to the tunnel axis. However, when the relative liner thickness is larger than a certain value, i.e., $t/a \ge 1.2$ and those points under investigation are in a range about $1 < r/a \le 1.5$ or $2 < r/a \le 3.5$, a maximum or minimum value of the radial displacement will occur when the distance to the tunnel axis reaches a certain magnitude for a given liner thickness (see Fig.10(a).

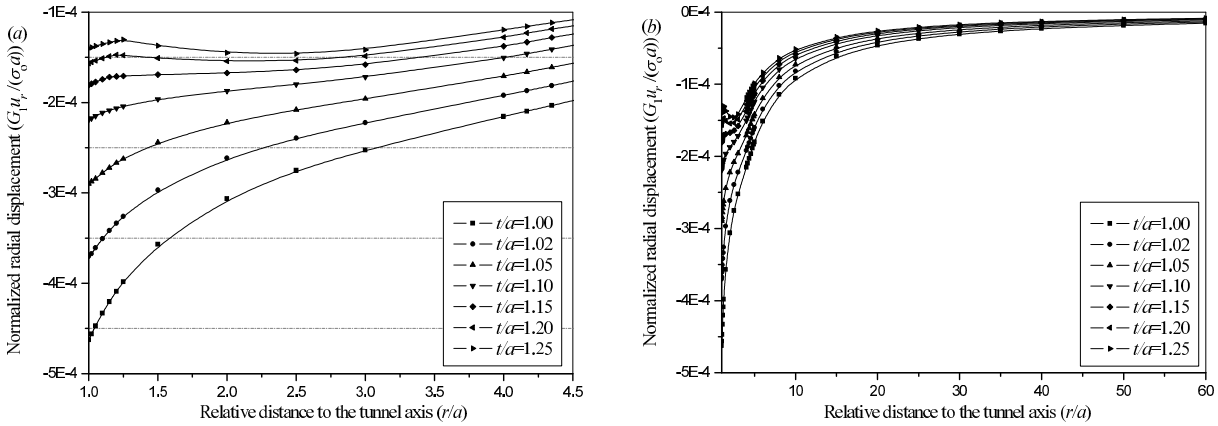

Figure 10 Variations of normalized radial displacement ($G_1u_r/(\sigma_o a)$) with relative distance to the tunnel axis (r/a) for various relative liner thicknesses (t/a) when $\Gamma = 10$.

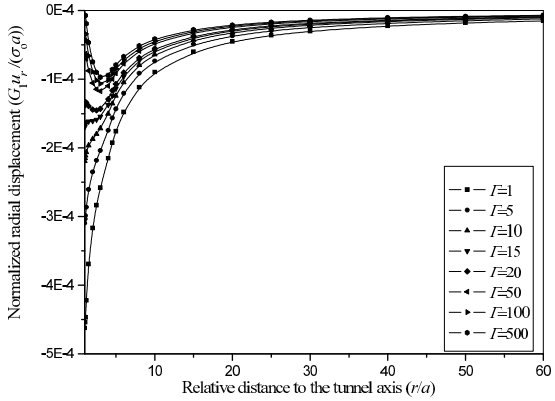

Figure 11 Variations of normalized radial displacement ($G_1u_r/(\sigma_o a)$) with relative distance to the tunnel axis (r/a) for various relative liner rigidities (Γ) when $t/a = 1.10$.

Fig.11 illustrates the variations of the normalized radial displacement with relative liner rigidity and distance to the tunnel axis when $t/a = 1.10$. It may be found that, when $\Gamma < 20$, y_r decreases monotonically with increasing r/a and t/a. However, if the relative liner rigidity $\Gamma \geq 20$ as shown in Fig.11, the varying trend of u_r is non-monotonic and u_r may obtain a negative maximum value when the distance to the tunnel axis reaches a certain value for a specific liner rigidity. It also be noted that, when $\Gamma \geq 50$, the radial displacement occurring at the inner boundary of the liner trends to 0.

Furthermore, it may be found from Figs.10 and 11 that in a range about $1 \leq r/a \leq 5$ the influences of the liner thickness and rigidity and the distance to the tunnel axis on the radial displacement are significant and when $20 < r/a$ the influences become insignificant. As for $r/a > 50$, Figs.10 and 11 indicate that the variations of the displacement field are almost independent of the values of r/a, t/a and Γ.

In Section 1 in the paper, the pressure tunnel is assumed that it is deep enough. However, Figs.6-9 indicate that, when those points under investigation are in the range of $r/a > 8$, the influence of tunnel excavation upon them is almost trivial. Thus, a conclusion may be drawn that, when the ratio between the embedded depth of a pressure tunnel and the outer radius of the liner is larger than 8, the results about the stress field in the paper are applicable for the stress analysis of the present tunnel. In addition, by comparing Figs.6-9 with Figs.10 and 11, it may be found that the influence of the tunnel excavation upon the displacement field is significantly larger than upon the stress field and only when the ratio between the embedded depth of a tunnel under investigation and the outer radius of the liner is larger than 50 the results about the displacement field in the paper are applicable for the displacement analysis of the tunnel.

5 CONCLUSIONS

In the present paper, an elastic stress-displacement solution for a deep pressure tunnel with impermeable liner in a saturated elastic porous geomaterial that obeys Terzaghi's effective stress principle is derived. The proposed solution considers the effects of the changes of the pore water pressure around the opening, the construction sequence of the tunnel and the interaction between the liner and the surrounding geomaterial on the mechanical response of the tunnel. Finally, the influences of the relative liner thickness and rigidity and the relative distance of the point under investigation to the tunnel axis on the stress-displacement fields for various combinations of the mechanical and geometric parameters are demonstrated numerically.

Acknowledgements The authors would like to deeply appreciate the financial support by the Project of Shandong Province Higher Educational Science and Technology Program (Grant No. J11LE03), the Natural Science Foundation of China (Grant No. 51009086), the Project supported by the Doctoral Foundation of Ludong University (Grant No. LY2011013), the Research Award Fund for Outstanding Middle-aged and Young Scientist of Shandong Province China (Grant No.BS2010HZ015) and the Program for Changjiang Scholars and Innovative Research Team in University (Grant No. IRT0843).

References

[1] F. Ahamad and R.Z. Mohammad. A theoretical solution for analysis of tunnels below groundwater considering the hydraulic-mechanical coupling. *Tunnelling and Underground Space Technology*, 24:634–646, 2009.

[2] M.A. Biot. General theory of three dimensional consolidation. *Journal of Applied Physics*, 12:155–164, 1941.

[3] A. Bobet. Analytical solutions for shallow tunnels in saturated ground. *Journal of Engineering Mechanics*, 127(12):1258–1266, 2001.

[4] A. Bobet. Effect of pore water pressure on tunnel support during static and seismic loading. *Tunnelling and Underground Space Technology*, 18:377–393, 2003.

[5] A. Bobet. Lined circular tunnels in elastic transversely anisotropic rock at depth. *Rock Mechanics and Rock Engineering*, 44:149–167, 2011.

[6] A. Bobet and S.W. Nam. Stresses around pressure tunnels with semi-permeable liners. *Rock Mechanics and Rock Engineering*, 40(3):287–315, 2007.

[7] B.H.G. Brady and E.T. Brown. *Rock mechanics for underground mining.* Allen & Unwin, 1985.

[8] W.I. Chou and A. Bobet. Predictions of ground deformations in shallow tunnels in clay. *Tunnelling and Underground Space Technology*, 17:3–19, 2002.

[9] H.H. Einstein and C.W. Schwartz. Simplified analysis for tunnel supports. *Journal of Geotechnical Engineering Division*, GT4:499–518, 1979.

[10] J.C. Jaeger, N.G.W. Cook, and R. Zimmerman. *Fundamentals of rock mechanics.* Blackwell Publishing, Oxford, 2007.

[11] G. Kirsch. Die theorie der elastizitat und die bedurfnisse der festigkeitslehre. *Zeitschrift des Vereines Deutscher In.genieure*, 42:797–807, 1898.

[12] S.W. Lee, J.W. Jung, S.W. Nam, and I.M. Lee. The influence of seepage forces on ground reaction curve of circular opening. *Tunnelling and Underground Space Technology*, 22:28–38, 2006.

[13] S.W. Nam and A. Bobet. Liner stresses in deep tunnels below the water table. *Tunnelling Underground Space Technology*, 21:626–635, 2006.

[14] F. Pellet, F. Descoeudres, and P. Egger. The effect of water seepage forces on the face stability of an experimental microtunnel. *Canadian Geotechnical Journal*, 30:363–369, 1993.

[15] H.G. Poulos and E.H. Davis. *Elastic solutions for soil and rock mechanics.* Wiley, New York, 1974.

[16] Y.J. Shin, B.M. Kim, J.H. Shin, and I.M. Lee. The ground reaction curve of underwater tunnels considering seepage forces. *Tunnelling and Underground Space Technology*, 25:315–324, 2010.

[17] Y.J. Shin, K.I. Song, I.M. Lee, and G.C. Cho. Interaction between tunnel supports and ground convergence – consideration of seepage forces. *International Journal of Rock Mechanics & Mining Sciences*, 48:394–405, 2011.

[18] K. Terzaghi. *Theoretical soil mechanics.* Wiley, New York, 1943.